Supporting Information

Tetrazolylpyrene Unnatural Nucleoside as a Human Telomeric Multimeric G-Quadruplex Selective Switch-On Fluorescent Sensor

Subhendu Sekhar Bag,* Manoj Kumar Pradhan and Sangita Talukdar

Bio-organic Chemistry Laboratory, Department of Chenistry, Indian Institute of Technology Guwahati, Guwahati-781039, Assam, India. Fax: (+)91-361-258-2349.
E-mail: ssbag75@iitg.ernet.in

1. General Spectroscopic Measurements

1.1. UV-visible measurements: UV-visible spectra of all the ODNs (2.5 µM concentration of each single strand) were measured in 50 mM sodium phosphate buffers (pH 7.0) containing 100 mM sodium chloride and 0.1 mM sodium-EDTA using Shimadzu UV-2550 UV-Visible spectrophotometer. with quartz optical cell of 1.0 cm path length and scanning rate of 0.5 nm with wavelength range of 200-500 nm and slit width of 2 nm.

1.2. Thermal melting temperature (T_m) experiments of the oligonucleotides: The thermal denaturation studies (T_m), absorbance vs. temperature profiles of the duplexes (2.5 µM concentration of each single strand) were measured at 260/280 nm using Shimadzu UV-2550 UV-Visible spectrophotometer equipped with a Peltier temperature controller using 1 cm path length cell in 50 mM sodium phosphate buffers (pH 7.0) containing 100 mM sodium chloride and 0.1 mM sodium-EDTA. The absorbance of the samples was monitored at 260 nm for duplexes and 280 nm for quadruplexes from 20 to 90 °C with a heating rate of 0.5 °C/min. From these profiles, average method was used to determine T_m values using in built software.

1.3. ***Steady state fluorescence experiments:*** ODNs solutions were prepared as described in UV-visible and T_m measurement experiments. Fluorescence spectra were recorded using Fluoromax–4 fluorescence spectrophotometer at 25 °C using quartz cell of 1.0 cm path length with a slit width of 3 nm, integration time 0.2 sec and wavelength range 300-600 nm. Excitation spectra were monitored at 307 (for single standed ODNs) and 319 nm (for duplexes) emission wavelength. Fluorescence emissions were collected exciting the ODNs at the wave length corresponding to their absorption maxima. Steady-state fluorescence emission spectra were recorded at room temperature as an average of five scans using an excitation slit of 3.0 nm, emission slit 3.0 nm, and scan speed of 120 nm/min. The steady state anisotropy experiment was performed with the same fluorescence spectrophotometer at 25 °C using 1 cm path length cell. The fluorescence anisotropy (r) was calculated using the following equation-

$$r = \frac{(I_{VV} - I_{VH}G)}{(I_{VV} + 2I_{VH}G)}\,;\; G = \frac{I_{HV}}{I_{HH}}$$

where, I_{VV} and I_{VH} are the emission intensities when the excitation polarizer is vertically oriented and the emission polarizer is oriented vertically and horizontally respectively. G is the correction factor. The terms I_{HV} and I_{HH} are the emission intensity when the excitation polarization is horizontally oriented and the emission polarization is oriented vertically and horizontally, respectively.

1.4. Circular dichroism (CD) measurement: CD spectra were recorded with JASCO CD J-810 spectropolarimeter equipped with a Peltier thermoelectric type temperature control system (2.5 µM concentration of each strand in 50 mM sodium phosphate, 100 mM sodium chloride, and 0.1 mM sodium-EDTA, pH 7.0, at room temperature).

The data were collected using quartz optical cells with a 1.0 cm path length. Measurements were conducted using 2.5 μM of strands in *T*m buffer. Corrections were made for buffer background CD spectra (200-400 nm) were recorded at 25 °C as an average of five scans and with a scan speed of 100 nm/min. The spectral data were analyzed with the spectra manager software.

2. Spectroscopic Properties for the Probe in presence and absence of various DNAs

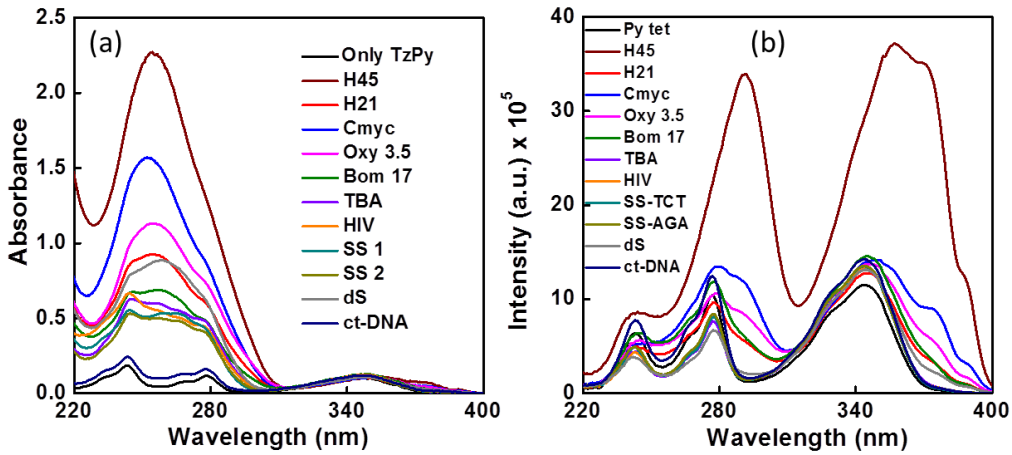

Figure S1. (a) UV-visible and (b) fluorescent excitation spectra of the probe nucleoside in presence and absence of various DNAs [All DNA concentration was 4 µM in 50 mM sodium phosphate buffer of pH 7, 100 mM NaCl and probe concentration was 10 µM].

Table S1. Photophysical summary of all DNA studied

Entry	λ_{abs}	$\Delta\lambda_{abs}$ [shift from 345 nm]	λ_{em}	$\Delta\lambda_{em}$ [shift from 402 nm]
$^{TzPy}B_{Do}$	345, 379	---	384, 402, 422	---
H45	356, 373, 390	11	394, 416	14
H21	348, 381	3	395, 416	14
Cmyc	351, 375, 389	6	395, 417	15
Oxy 3.5	350, 375	5	395, 416	14
Bom 17	348, 379	3	394, 415	13
TBA	347, 379	2	385, 404,424	2
HIV	347, 379	2	385, 404,424	2
SS1	347, 380	2	384, 404, 423	2
SS2	347, 380	2	384, 404, 423	2
dS	349, 377	4	395, 417	15
ct-DNA	347, 381	2	384, 404, 423	2

3. Spectroscopic Properties for the Probe in presence of H45 DNA

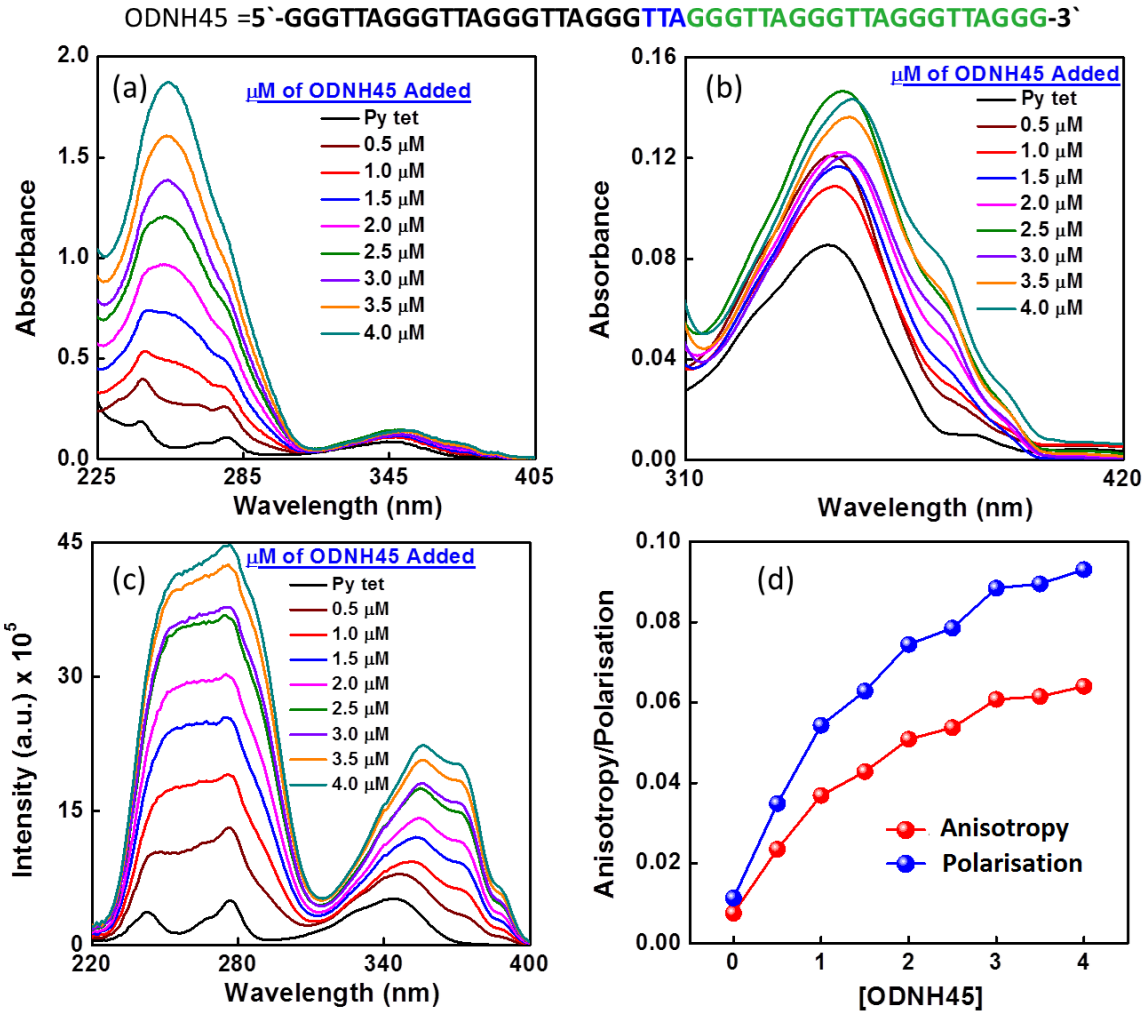

Figure S2: (a-b) UV-visible and (c) fluorescence excitation titration (λ_{em} = 400 nm), (d) fluorescence anisotropy spectra of the probe in presence of various concentration of H45 DNA [50 mM sodium phosphate buffer of pH 7, 100 mM NaCl and probe concentration was 10 μM].

Table S2. Photophysical summary of **H45** with $^{TzPy}\mathbf{B_{Do}}$.

μM of H45	λ_{abs}	$\Delta\lambda_{abs}$ [shift from 344 nm]	λ_{em} (λ_{ex} = 370 nm)	$\Delta\lambda_{em}$[shift from 383 nm]
$^{TzPy}\mathbf{B_{Do}}$	344	---	383, 404	---
0.5	349, 377	5	395, 416	12
1.0	350, 377	6	395, 416	12
1.5	351, 376	7	395, 416	12
2.0	351, 375	7	395, 416	12

2.5	351, 375	7	395, 416	12
3.0	353, 375	9	395, 416	12
3.5	354, 373	10	395, 416	12
4.0	335, 372	11	395, 416	12

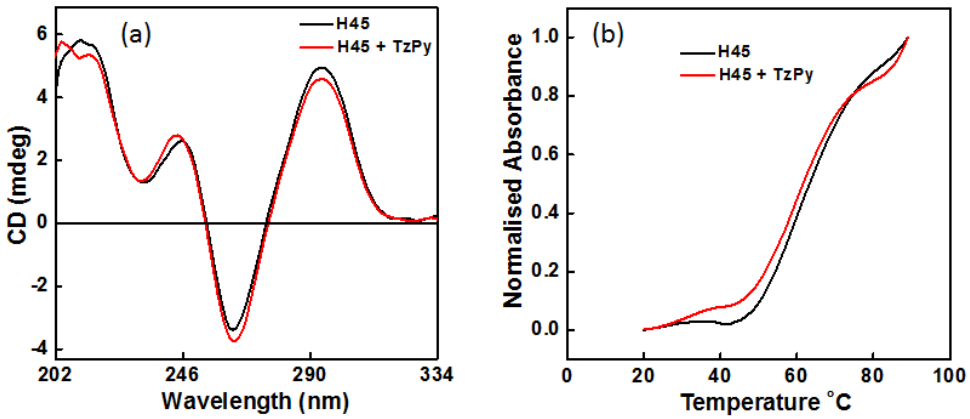

Figure S3: (a) CD spectra and (b) thermal melting graph of H45 DNA in presence of the probe.

4. Spectroscopic Properties for the Probe in presence of H21 DNA

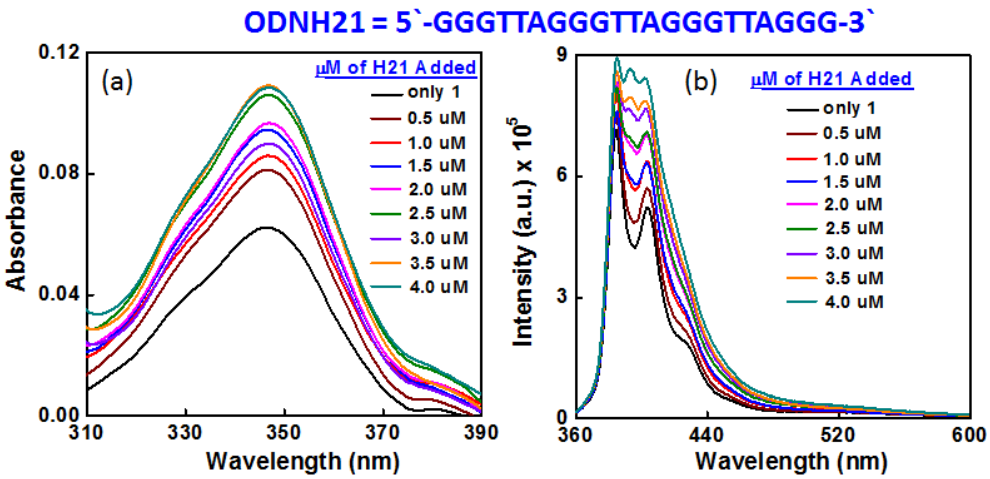

Figure S4: (a) UV-visible and (b) fluorescence titration spectra of the probe in presence of various concentration of H21 DNA [50 mM sodium phosphate buffer of pH 7, 100 mM NaCl and probe concentration was 10 µM].

Table S2. Photophysical summary of H21 with TzPy.

μM of H21	λ_{abs}	$\Delta\lambda_{abs}$	λ_{em}, (λ_{ex} = 350 nm)	λ_{em}, 280 nm	$\Delta\lambda_{em}$
$^{TzPy}\mathbf{B_{Do}}$	344, 379	---	384, 403	383, 403	---
0.5	347, 380	3	384, 403	383, 402	---
1.0	348, 380	4	384, 403	383, 402	---
1.5	348, 380	4	384, 403	392	9
2.0	348, 380	4	385, 402	392, 413	9
2.5	348, 380	4	385, 402	393, 413	10
3.0	348, 380	4	385, 401	393, 413	10
3.5	348, 380	4	385, 401	393, 414	10
4.0	348, 380	4	385, 401	393, 414	10

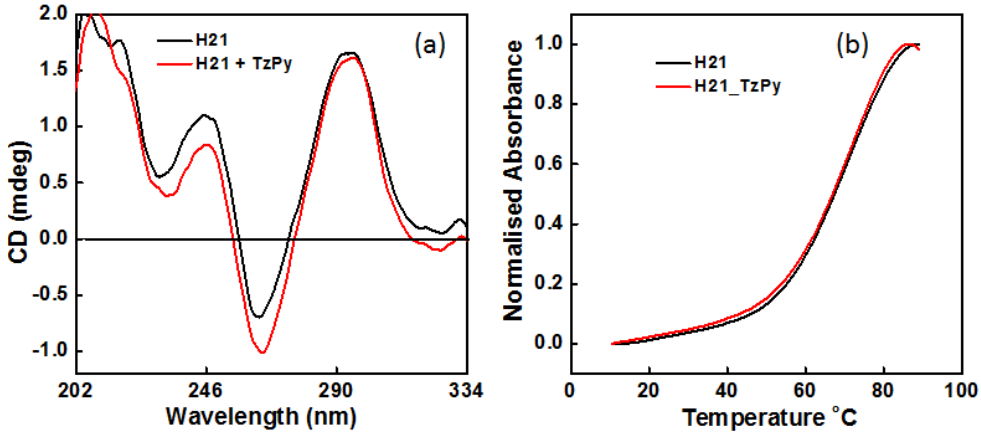

Figure S5: (a) CD spectra and (b) thermal melting graph of H21 DNA in presence of the probe.

5. Docking study for the Probe in presence of H45 DNA

Two high-resolution NMR structures for the human telomeric G-quadruplexes, Hybrid 1 and Hybrid 2, reported by Phan, Patel and coworkers[1] were used as building blocks. From these two monomeric motifs, the dimeric **H 45** model G-quadruplex (formed by a Hybrid 1 G-quadruplex at 5´-end and a Hybrid 2 G-quadruplex at the 3´-end) was constructed following literature reports by Chaires et al.[2] and **Huang** et al.[3] Subsequently, this dimeric **H 45** model G-quadruplex was used as host in docking study using AutoDock 4.2 programme. [4] We also optimised the ligand (the probe nucleoside, $^{\mathbf{TzPy}}\mathbf{B_{Do}}$) at B3Lyp/6-31G* level of theory using G09 programme package.[5] To test accuracy of the docking results, the docking process was repeated three times. The AutoDock tools (ADT) were utilised for charges and polar hydrogens addition as well as for setting the other parameters. AutoGrid 4.0 and AutoDock 4.0 were used to produce grid maps. A grid box to a size of 60 × 60 × 60 with 0.375 Å spacing was generated. Total grid points per map were 226981. The centre grid box for x-, y- and z centres were 11.388, -4.907, and 1.479 with offsets 1.694, 0.806 and 0.667, respectively. In the prescriptive grid box, we calculated the complex conformation with flexible molecular docking method. The Lamarckian genetic algorithm (LGA) [4a] was choosen to carry out a flexible molecular docking of the small molecules to the receptor and to calculate the complex conformation. The other items used were the default settings. A total of 10 conformations from each docking were obtained and the least binding energy was considered as the best-docked conformation. Further intermolecular-hydrophobic, polar and hydrogen bond interactions were analysed using PyMOL.[6] The probe nucleoside $^{\mathbf{TzPy}}\mathbf{B_{Do}}$ did not perturb the topology of multimeric telomeric G-quadruplex **H 45.**

1. Anh Tuân Phan, Vitaly Kuryavyi, Kim Ngoc Luu, and Dinshaw J. Patel *Nucleic Acids Res.* 2007 35, 6517.
2. Petraccone,L., Trent,J.O., Chaires,J.B. *J. Am. Chem. Soc.*, 2008, **130**, 16530–16532.
3. (c) Ming-Hao Hu, Shuo-Bin Chen, Bo Wang, Tian-Miao Ou, Lian-Quan Gu, Jia-Heng Tan, Zhi-Shu Huang, *Nucleic Acids Res.*, 2017, 45, 1606.
4. (a) G.M. Morris, David S. Goodsell, R.S. Halliday, R. Huey, W.E. Hart, R.K. Belew,Automated docking using Lamarckian genetic algorithm and an empiricalbinding free energy function, J. Comput. Chem. 19 (1998) 1639–1662.(b) G.M. Morris, R. Huey, W. Lindstrom, M.F. Sanner, R.K. Belew, et al., AutoDock4and AutoDockTools4: Automated docking with selective receptor flexibility, J.Comput. Chem. 30 (2009) 2785–2791.
5. Frisch, M. J. et al., G09, Gaussian, Inc. Wallingford CT, **2009**.
6. (a) Pratibha Singh, Priti Talwar *J. Mol. Graph. Model.* 2017, 77, 153–167. (b) A.M. Vijesh, Arun M. Isloor, Sandeep Telkar, T. Arulmoli, Hoong-Kun Fun, *Arab. J. Chem.* 2013, 6, 197.

CLUSTER ANALYSIS OF CONFORMATIONS

Number of conformations = 10

RMSD cluster analysis will be performed using the ligand atoms only (31 / 31 total atoms).

Outputting structurally similar clusters, ranked in order of increasing energy.

Number of distinct conformational clusters found = 3, out of 10 runs, Using an rmsd-tolerance of 2.0 A

Table S3. CLUSTERING HISTOGRAM

Cluster Rank	Lowest Binding Energy	Run	Mean Binding Energy	Num in Clus	Histogram 5 10 15 20 25 30 35
1	-9.07	2	-8.90	3	###
2	-9.00	8	-8.62	5	#####
3	-8.37	3	-8.36	2	##

Table S4. Various interaction of **H45** with $^{TzPy}B_{Do}$.

G-quadruplex Units	Residues	Probe Nucleoside Moiety	Interactions	Distances (Å)
G-quadruplex unit 1	DG 6	Pyrene	π--π-Stacking	4.77
	DT 14	Pyrene	π--π-Stacking	5.44
	DA 15	Triazol	T-shaped π--π-stacking	3.88
	DA 15	Triazol-N1/N2	Electrostatic	3.00/2.90
	DG24	Pyrene	π--π-Stacking	4.17
TTA Loop	DT 25	Pyrene	π--π-Stacking	3.32
	DT 26	Pyrene	π--π-Stacking	4.21
	DA 27	Pyrene	π--π-Stacking	4.67
G-quadruplex unit 2	DA 27 (N7)	Sugar-5'-OH	Electrostatic	3.45
	DA 27 (C6-NH2)	Sugar-5'-OH	Electrostatic and H-bonding	3.13
	DT 38	Pyrene	π--π-Stacking	5.89
	DA 39	Pyrene	π--π-Stacking	3.56
	DA 39 (N1)	Sugar-5'-OH	Electrostatic	2.71
	DA 45	Triazole	π--π-Stacking	5.05
	DG 46 (Sugar-O4')	Sugar-3'-OH	H-bonding	2.01

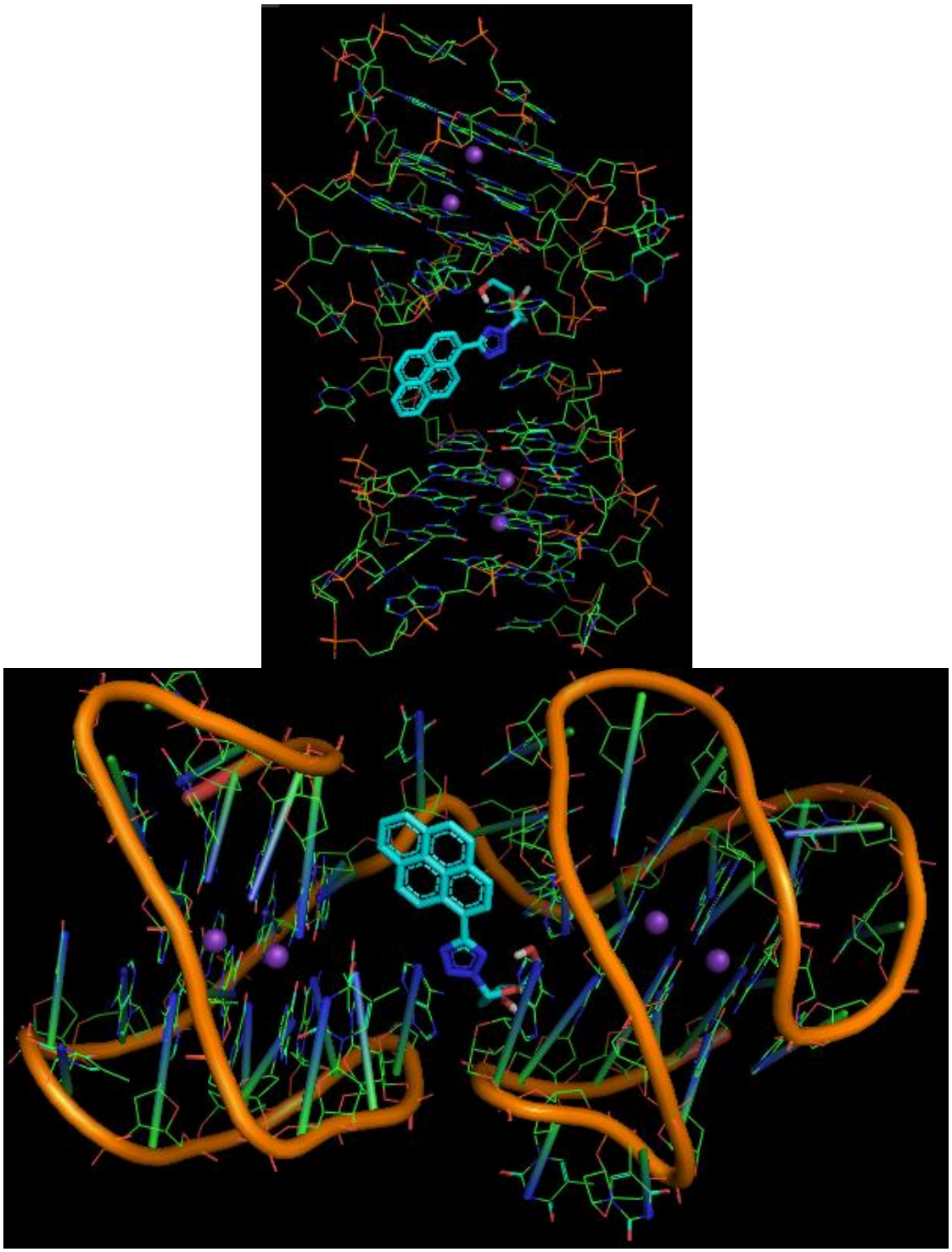

Figure S6: The docking poses of the nucleoside probe with multimeric **H45** G-quadruplex.